Materials Advances

Accepted Manuscript

This article can be cited before page numbers have been issued, to do this please use: A. Bellil, A. Aziz, K. Felaous and A. Driouich, *Mater. Adv.*, 2026, DOI: 10.1039/D5MA00680E.

ROYAL SOCIETY OF CHEMISTRY

rsc.li/materials-advances

View Article Online
DOI: 10.1039/D5MA00680E

Thermal stability and physico-mechanical assessment of volcanic pozzolan-based concrete at elevated temperatures

Abdelilah Bellil[1], Ayoub Aziz[1]*, Khadija Felaous[1], Anas Driouich[2]

1. Scientific Institute, Mohammed V University in Rabat, Morocco
2. Laboratory of Process Engineering and Environment, Faculty of Sciences and Technology, University Hassan II, Mohammedia, Morocco

* Corresponding author: Pr. Ayoub AZIZ
E-mail address: Ayoub.aziz2@um5.ac.ma

View Article Online
DOI: 10.1039/D5MA00680E

Abstract

The development of sustainable construction materials with high fire resistance is a critical challenge in civil engineering. This experimental study investigates the synthesis, characterization, and high-temperature performance of lightweight concrete produced with natural volcanic pozzolan aggregates. Conventional fine and coarse aggregates were partially or fully replaced with volcanic pozzolan at rates of 0 % (CPz0), 25 % (CPz25), 50 % (CPz50), 75 % (CPz75), and 100 % (CPz100). Specimens were exposed to temperatures ranging from 25 °C to 800 °C to assess the impact of thermal treatment on their physico-mechanical properties. The results indicate that thermal degradation primarily affects concretes containing conventional limestone aggregates (CPz0 and CPz25), with the formation of microcracks and damage at the paste–aggregate interface observed from 400 °C. Mass loss and compressive strength reductions were strongly correlated with the principal components identified through Principal Component Analysis (PCA). Increasing the substitution rate with volcanic pozzolan improved thermal stability and preserved mechanical performance, even at elevated temperatures where limestone-based concretes exhibited significant degradation. These findings demonstrate the feasibility of using natural volcanic pozzolan to produce fire-resistant concretes, offering a promising solution for durable and high-performance construction applications in thermally demanding environments.

Keywords: Volcanic pozzolan; concrete; high-temperature; thermal resistance; durability.

1. Introduction

The surge in population growth in recent years has brought concrete to the forefront as one of the most extensively used construction materials [1]. This popularity is rooted in its significant characteristics, such as robust mechanical properties, exceptional durability, workability, and resistance to fire [2]. Concrete's adaptability is a key feature, allowing it to be molded into various shapes for diverse architectural and structural applications. Noteworthy is its low thermal conductivity and non-combustible nature, making it a more inert material when compared to alternatives like wood and steel [3]. Despite its widespread application in construction, concrete faces a significant risk of mechanical deterioration and potential structural degradation when subjected to elevated temperatures [3].

In the field of construction and materials engineering, fire is a major hazard to building components. When exposed to high temperatures, concrete structures and their microstructure are negatively impacted, affecting their properties. To guarantee the safety of the structure and its occupants, improving concrete's fire behavior is one of the crucial steps. Janotka. I et al [4]

View Article Online
DOI: 10.1039/D5MA00680E

demonstrated that at high temperatures, concrete specimens exhibit cracking, weight loss, strength reduction, and modulus of elasticity. When exposed to high temperatures, the main factors that influence the strength of concrete are the type of aggregate, moisture content, and the heating and cooling down process [5]. Yüksel I [6] asserts that the fire resistance of concrete is subject to multiple influencing factors, encompassing the type of cement and aggregate employed, the structural element's dimensions, the duration of heat exposure, and the moisture content within the concrete. The selection of appropriate aggregates for concrete production is very important to achieve high performance [7].

Various research [8–10], have been directed to evaluate the influence of aggregate type on the performance of concrete at high temperatures. Turker et al [11] reported that concrete using pumice as coarse aggregate had better interfacial conditions than concrete using granite and limestone coarse aggregate. In addition, Neville [12] reported that at temperatures above the approximate value of 430°C, the strength of concrete using granite aggregates begins to decrease sharply, unlike concrete using lightweight aggregates.

Natural volcanic pozzolan aggregate (PA) is a porous aggregate type that can be utilized in the production of concrete with a comparatively lower density compared to traditional concrete, along with a high thermal insulation capacity [13,14]. Volcanic pozzolan, a silico-aluminous volcanic rock, displays a distinctive vacuolar structure and vitreous texture [15]. This morphology is a consequence of its genesis via the aerial projection of lava fragments enriched with gas, experiencing swift cooling during the eruptive phases of volcanic gas expulsion [16]. In the literature, PA could be used in the production of concrete instead of coarse aggregate and cement when finely ground [13,17,18]. In other studies, natural pozzolan is also used in geopolymers [19–24] and ceramic membranes [25,26].

Based on the experimental work carried out to date, no study has addressed the thermal stability of normal concrete containing natural volcanic pozzolan aggregates. Consequently, this study examines the impact of elevated temperatures on the physical and mechanical performance of concrete produced with different proportions of volcanic pozzolan aggregates.

The present study focuses on the synthesis and characterization of a high-temperature resistant concrete based on a natural volcanic rock. The raw materials were first characterized geochemically, mineralogically and thermally. Various concrete formulations were then produced, progressively replacing fine and coarse limestone aggregates with volcanic pozzolan aggregates. After the age of curing, the synthesized specimens were exposed to different temperatures (200, 400, 600, and 800°C) and their physico-mechanical, thermal, and microstructural properties were determined using several analytical techniques: macroscopic

View Article Online
DOI: 10.1039/D5MA00680E

stability, mass loss, shrinkage, mechanical strength, optical microscopy, and P-wave velocity in the specimens. Finally, a statistical study using the principal component analysis method (PCA) was carried out to determine the interactions between sample exposure temperature and the parameter responses found.

2. Materials and experimental approach

2.1 Materials

Binder: The cement used in this work to formulate the concrete is a Portland cement, type CPJ-45, manufactured by LafargeHolcim in Morocco. This cement conforms to Moroccan standard NM10.1.004 [27]. The material features an absolute density of 3100 kg/m^3, a bulk density of 1100 kg/m^3, and a specific fineness of 3200 cm^2/g. Detailed information regarding its chemical composition is presented in Table 1.

Table 1. Chemical analysis by XRF of cement and natural pozzolan.

Oxides %	SiO_2	Al_2O_3	Fe_2O_3	CaO	K_2O	MgO	TiO_2	SO_3	Na_2O
Cement CPJ 45	21.30	5.58	3.40	62	2.10	1.85	0.30	2.41	-
Natural pozzolan	45.92	18.42	10.28	9.39	1.57	6.82	-	-	3.69

Fin aggregates (Beach sand): The sand used in this work comes from the Mehdia sand deposit located in northwest Morocco (34°09'16.56 “N; 6°43'54.70” W), near the town of Kénitra (Fig. 2). The Mehdia sands were formed during the Quaternary, the last geological period, marked by cycles of glaciations and interglaciations. During this period, sand grains were transported by ocean currents along the coast. The prevailing currents in the region favored the southward movement of sand, gradually accumulating it to form the vast beaches observed at the present time. Changes in sea level and climatic variations have had a significant impact on sand erosion, transport and sedimentation, contributing to the shaping of the current landscape [28]. Sampled sand was washed, dried, sieved to a particle size of 0.08/2 mm, and used as fine aggregate.

Coarse aggregates (Limestone): The conventional aggregate used in this work is a reef limestone from Ain Jemaa located in the Rabat-Salé-Kénitra region (33°33'12 “N; 6°04'13 ”W) (Fig. 2). The Ain Jemaa reef limestones were formed during the Devonian, and more precisely the Eifelian and Givetian, in a shallow marine environment characterized by clear, warm waters. The reefs were made up of a variety of marine organisms, including corals, algae, bryozoans, and foraminifera. These organisms contributed to the construction of reef structures and the production of carbonates [29]. The limestone sample was crushed to a size of 2/12 mm and used as coarse aggregate.

View Article Online
DOI: 10.1039/D5MA00680E

Coarse aggregates (volcanic pozzolan): The volcanic aggregates used in this work are the volcanic pozzolans of the Boutagerouine volcanic complex in the central Middle Atlas volcanic region (33.28879° N, -5.082962° W) (Fig. 2). It is a volcanic complex formed in the Middle MioPlio-Quaternary geological time by elements of eight juxtaposed cones of varying size, with an overall height of 150m and a width ranging from 2000m to 4500m. This large volcano is formed by the accumulation of a large volume of lapilli and bombs during several synchronous eruptions. This configuration reflects a synchronism between strombolian and phreatomagmatic dynamics during eruption initiation [14]. The pozzolan fragements sampled were crushed and sieved to two particle sizes (0.08/2 and 2/12 mm) and used as fine and coarse aggregates (Fig. 1). Scanning electron microscopy images show a porous structure in the pozzolan, with both open and closed pores (Fig. 1), characteristic of its volcanic origin. This microstructure contributes to its low thermal conductivity and stable behavior at high temperatures.

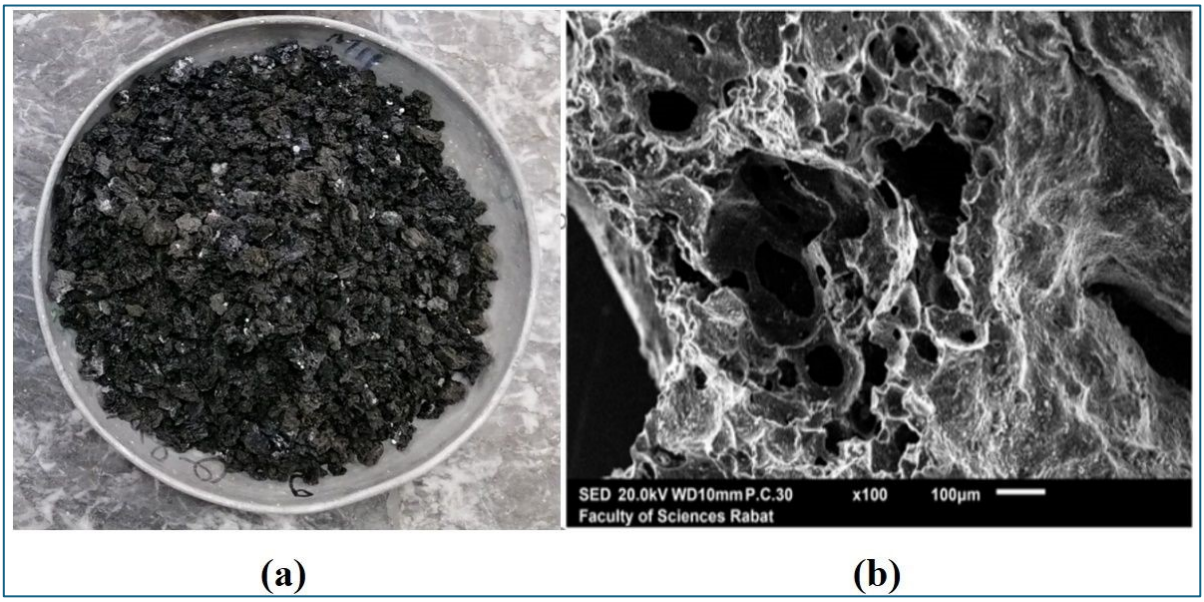

Fig. 1. Macroscopic aspect of pozzolan, b) Microscopic aspect of pozzolan obtained by SEM.

Water: The concrete was mixed using potable water that adhered to the physical and chemical standards outlined in NM 10.1.353 standards [23].

View Article Online
DOI: 10.1039/D5MA00680E

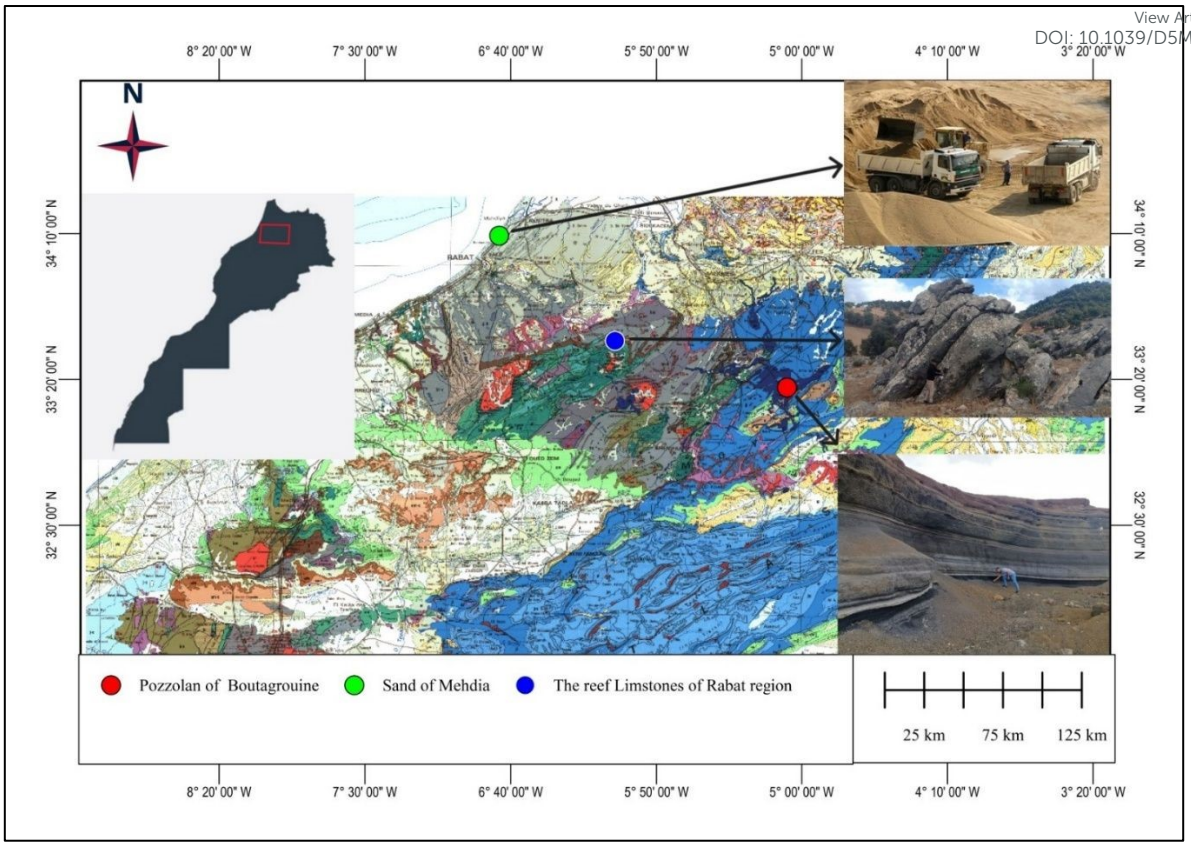

Fig. 2. Geographic location and photos of the studied geomaterial quarries.

2.2 Mix design and specimen preparations

The methodology adopted in this study is schematically shown in Fig. 3. After pre-treating the raw material, concrete formulations were prepared by simultaneously replacing conventional fine and coarse aggregates with volcanic pozzolan aggregates in the proportions shown in Table 2. For each formulation, the binder, fine and coarse aggregates, and superplasticizer were mixed with water, at a W/C ratio of 0.55, using a mixer for 3 min. To control the W/C ratio during mixing, pozzolan aggregates, which have a highly absorbent nature, were immersed in water for 24 hours, then drained for around 30 minutes until their surface moisture became constant. The resulting batches of fresh concrete were then poured into cubic ($10 \times 10 \times 10$ cm^3) and prismatic ($4 \times 4 \times 16$ cm^3) molds and exposed to vibration using a vibrator plate. After 24 h, the samples were removed from their molds and emerged for 28 days in water to ensure complete hydration.

After 28 days, the obtained specimens were oven-dried and exposed to different temperatures (200, 400, 600, and 800°C) using a heating rate of 5 °C/min. Once the target temperature had been reached, the samples were subjected to a residence time of 1 hour to reach thermal

View Article Online
DOI: 10.1039/D5MA00680E

equilibrium. Once heat exposure was complete, the samples were cooled gradually to avoid thermal shock and stored to determine their physico-mechanical properties.

Table 2. Mixing design and material amounts.

Blended ID	Replacement rate (%)	Cement (Kg/m³)	Mehdia Sand (Kg/m³)	Limestone aggregates (Kg/m³)	Pozzolan sand (Kg/m³)	Pozzolan aggregates (Kg/m³)
CPz0	0	400	784	1175	0	0
CPz25	25	400	588	881	149	171
CPz50	50	400	392	588	295	342
CPz75	75	400	196	294	442	512
CPz100	100	400	0	0	588	682

**CPzX-TY: X the replacement rate of CA by PA; Y the concrete exposure temperature.*

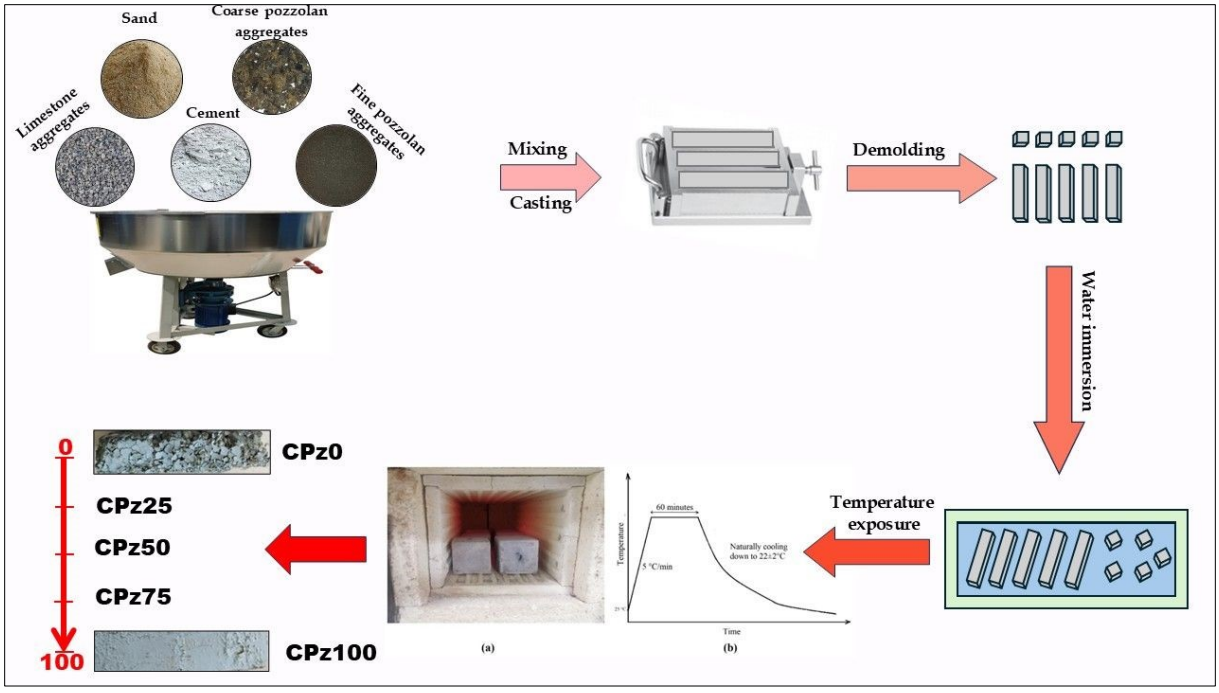

Fig. 3. Schematic diagram of the experimental procedures carried out in this study

2.3 Testing methods

The chemical composition of the raw materials was analyzed using X-ray fluorescence (XRF) with an Axios PANalytical spectrometer. The morphology of the pozzolan was observed using a Jeol TSM-IT100 scanning electron microscope (SEM) operating at 20 kV.

View Article Online
DOI: 10.1039/D5MA00680E

The fire resistance tests were performed according to ASTM E119 using a controlled furnace equipped to follow the standard temperature-time curve. Specimens were exposed to temperatures up to 800 °C at a heating rate of 5 °C/min.

To evaluate thermal degradation, the mass loss of concrete specimens was calculated based on the average of three cubic samples measuring 40 x 40 x 160 mm³, using the following equation:

$$\text{Loss of mass (\%)} = \frac{m_1 - m_2}{m_1} \times 100$$

Where, the variable m_1 and m_2 denote the mass before and after heating, respectively.

The compressive strength of the specimens was tested according to ASTM C39 utilizing a standardized machine (Controlab) with a capacity of 250 kN (Fig. 4 (a)). The loading rate was set at 0.5 MPa/s.

The ultrasonic pulse velocity (UPV) measurement was made by non-destructive digital indication tester equipment (Fig. 4 (b)) according to ASTM C597-09 to evaluate changes in pore distribution and cracking caused by heat exposure. UPV values were performed on prismatic samples with a dimension of 40 × 40 × 160 mm³ after exposure to the target temperatures.

(a) (b)

Fig. 4. Illustration of (a) compressive strength test; (b) UPV test apparatus.

The statistical analysis was conducted using the Principal Component Analysis (PCA) method, which serves as a data analysis tool by explaining the correlation or covariance structure

View Article Online
DOI: 10.1039/D5MA00680E

through linear combinations of the original variables. Utilizing PCA allows for the reduction and interpretation of data within a constrained space [30,31]. In the present study, the utilization of PCA is directed towards representing the utmost information from the initial data in the form of a biplot [31]. We performed statistical processing using SPSS version 26 soft.

3. Results and discussions

3.1 Appearance following exposure to elevated temperatures

The surface analysis of specimens following exposure to various target temperatures was investigated, and the resultant images are depicted in Fig. 5. As the temperature increases, the color transformation in each set of specimens progresses from a light gray hue at 200 °C to gray at 400 °C, transitioning to light pink at 600 °C, and ultimately reaching gainsboro gray at 800 °C. These findings align with existing literature [32].

In all samples, no significant cracks were observed throughout the temperature range of 25-400 °C. Upon reaching a temperature exposure of 600 °C, minor cracks and surface crazing became visible on the surface of samples CPz-0 and CPz-25. This is attributed to the pore pressure built up by the conversion of moisture to vapor [33]. Similarly, minor random cracks were observed on the surface of samples Cpz-50 and CPz-75 and some micro-cracks on Cpz-100. Upon increasing the furnace temperature to 800 °C, specimens CPz-0 and CPz-25 exhibited significant degradation, with visible cracks and coarse fissures. After 48 hours, further internal cracking propagated to the surface, resulting in substantial concrete failure. This delayed cracking is mainly attributed to the presence of CaO in the limestone aggregates, which absorbs ambient moisture through microcracks and transforms into portlandite ($Ca(OH)_2$) within the cement matrix [34]. Therefore, further testing of specimens CPz-0 and CPz-25 was limited up to 600 °C. In contrast, at 800 °C, no spalling was observed in the specimens CPz-50 CPz-75 and Cpz-100, due to the porous microstructure of the specimens that allows unimpeded water vapor loss.

View Article Online
DOI: 10.1039/D5MA00680E

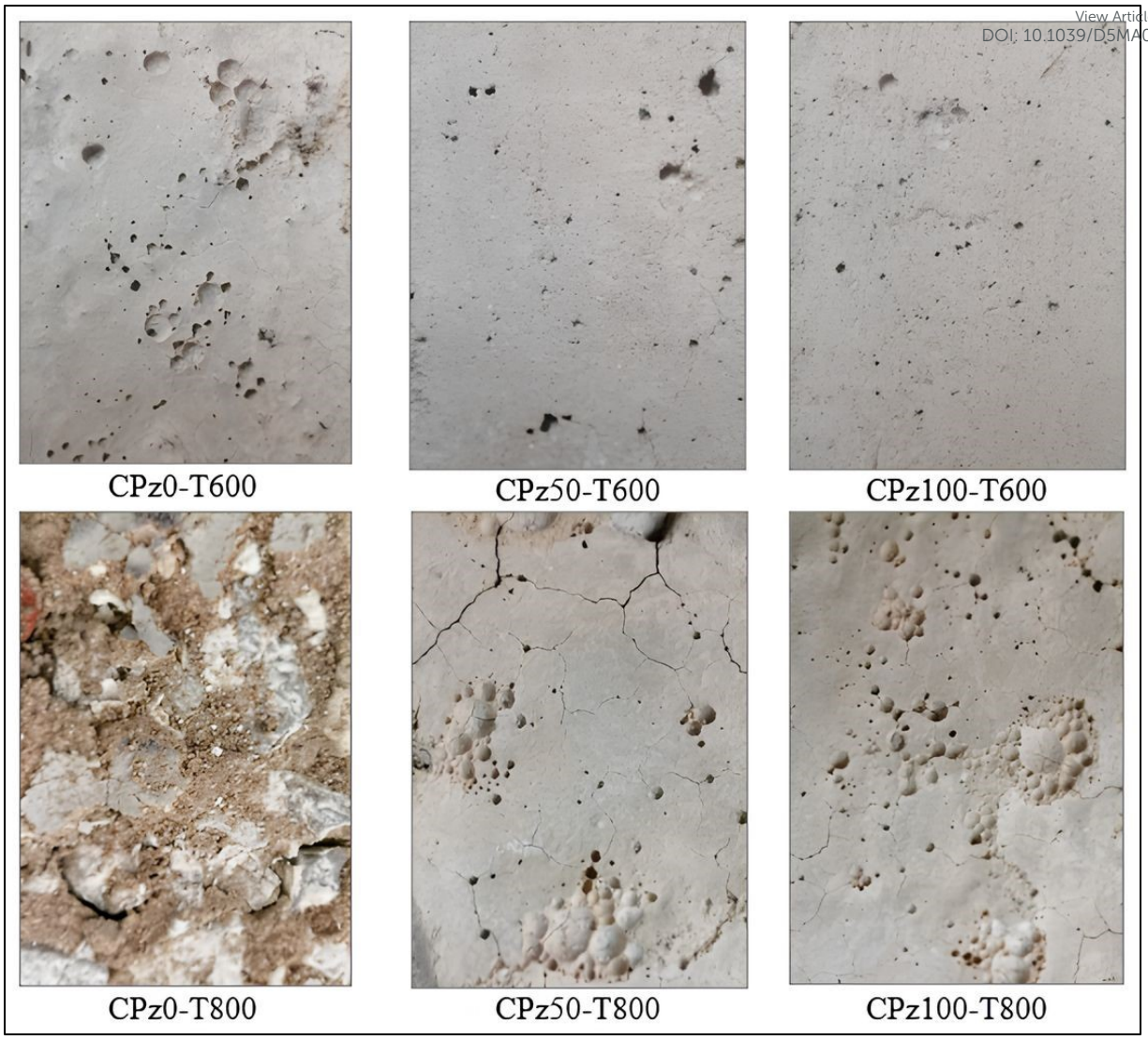

Fig. 5. The surface appearance of samples after exposure to 600 °C and 800 °C.

3.2 Mass loss

The mass loss values exposed at different temperatures are shown in Table 3 in %. For all series, mass loss shows the same trend. In fact, mass loss increases with increasing temperature [8], as well as with increasing replacement of natural aggregates by PA. Moreover, as temperature continues to rise, the rate of mass decay becomes progressively less significant for all samples examined. The mass loss observed in the concrete samples is essentially the result of two phenomena: the disappearance of free water generated during heating, and the dehydration of the hydrated tricalcium silicate and ettringite phases [11,32]. At a temperature of 200 °C, concrete mixes CPz-25, CPz-50, CPz-75, and CPz-100 recorded mass loss reductions of 3.75%, 5.35%, 6.44%, and 6.89% respectively, while the reference mix CPz-0 showed a decrease of only 2.12%. This significant reduction is mainly attributable to the high porosity of PA, resulting in more pronounced water absorption than natural aggregates (NA).

View Article Online
DOI: 10.1039/D5MA00680E

Generally, the primary factors contributing to mass loss up to 400°C were the evaporation of excess water and the dehydration processes involving C-S-H, AFt, and AFm. [35]. Beyond that temperature range, mass loss was primarily attributed to the decomposition of $Ca(OH)_2$ [36]. Furthermore, as the temperature continues to rise, the rate of mass reduction becomes progressively less significant for all tested samples [35].

Table 3. Evolution of mass loss of concrete as a function of temperature.

	200°C	400°C	600°C	800°C
CPz-0	2.12	5.42	6.21	--
CPz-25	3.75	5.64	6.77	--
CPz-50	5.35	6.54	7.27	7.34
CPz-75	6.44	7.21	7.66	7.81
CPz-100	6.89	7.72	8.05	8.07

3.3 Compression test results

Fig. 6 shows the effect of replacing natural aggregates with natural pozzolan aggregates on the compressive strength of concrete at different temperatures. It can be seen that the compressive strength of the samples after high temperatures deteriorates significantly with increasing temperature. Moreover, all series show the same trend of variation before and after elevated temperatures. As shown in Figure 6, when the contents of pozzolan aggregates are 0%, 25% 50%, 75%, and 100%, the respective compressive strength values of the simples at ambient temperature are 41.54 MPa, 37.47M MPa, 31.27 MPa, 28.26MPa, and 25.66 MPa respectively. Which means that, when pozzolan aggregates replace natural coarse and fine aggregates in concrete, they do not resist pressure like natural aggregates due to of the elevated porosity of PA, and therefore it will ultimately leads to a reduction in compressive strength [13].

View Article Online
DOI: 10.1039/D5MA00680E

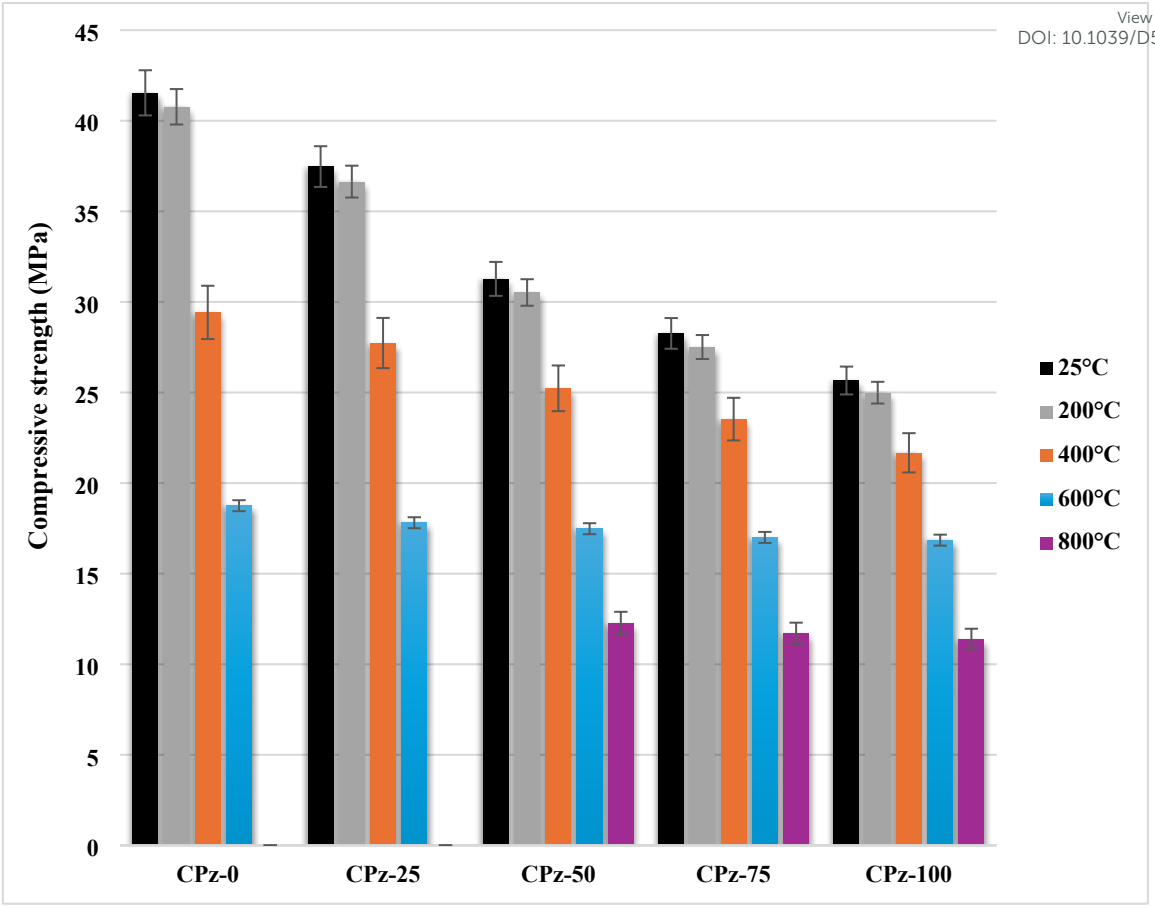

Fig. 6. Compressive strength of specimens exposed to elevated temperatures, at 28 days.

The results obtained in Fig. 7 show the evolution of the loss of compressive strength during the heating cycle of the samples studied. It can be seen that, the difference between the initial and final compressive strength was reported as a percentage loss in strength. Furthermore, the results show that at all exposure temperatures, the loss of strength diminishes as the substitution rate of PA with NA rises from 0% to 100%. At 200 °C exposure, a slight reduction in specimen compressive strength was observed for all concretes (less than 3%). In addition, beyond 200 °C, it becomes apparent that an increase in the pozzolan percentage results in a less significant decline in compressive strength as the temperature rises. Moreover, the lowest rate of strength reduction was observed for CPz-100 specimens at 800 °C, while the highest was observed for CPz-0 and CPz-25 specimens. This behavior is consistent with observations reported in the literature, where concretes made with limestone aggregates exhibit a significant reduction in compressive strength beyond 600 °C due to the thermal degradation of hydrated phases and carbonate aggregates, resulting in substantial mechanical performance loss at 650 °C and above [37]. This improvement using pozzolan aggregates can be explained by a stronger bond between the cement paste and the porous pozzolan aggregates compared to calcareous aggregates,

View Article Online
DOI: 10.1039/D5MA00680E

enhancing the concrete's mechanical performance at elevated temperatures [38], along with the quantity of aluminum present in the pozzolan aggregate. Therefore, the higher the pozzolan aggregate content in the concrete, the better the strength retention at high temperatures. We find that concrete produced with PA has good performance in terms of strength preservation.

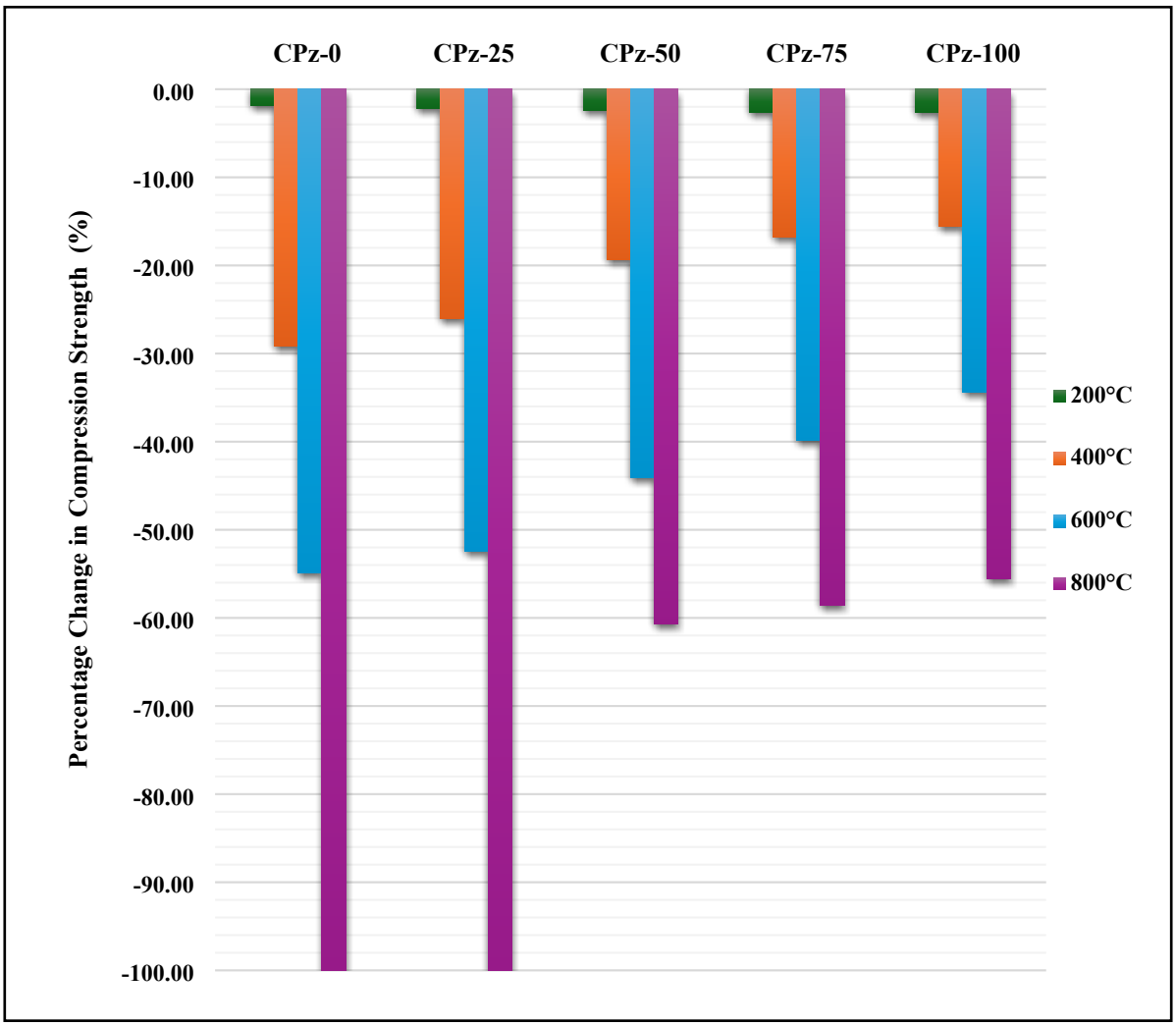

Fig. 7. Variation of compressive strength of concrete with temperature, at 28 days.

3.4 Ultrasonic pulse velocity

The Ultrasonic pulse velocity method (UPV) has been extensively employed for assessing concrete quality. The ultrasonic pulse velocity in concrete is impacted by any changes in the concrete; thus, it is influenced by the proportions of the concrete mix [39]. The results of the evolution of UPV in concrete mixes are presented in Figure 8. It is shown that the UPV decreases with an increase in temperature, aligning with findings in the existing literature. [40,41].

View Article Online
DOI: 10.1039/D5MA00680E

The UPV at ambient temperature decreases with the increasing rate of replacement of natural aggregates by pozzolan aggregates. This decrease can be attributed mostly to the amount of air voids trapped due to the PA in the mixtures [13]. At 200 °C, the measured ultrasonic pulse velocity did not change significantly. However, the UPV tended to decrease once above 200 °C.

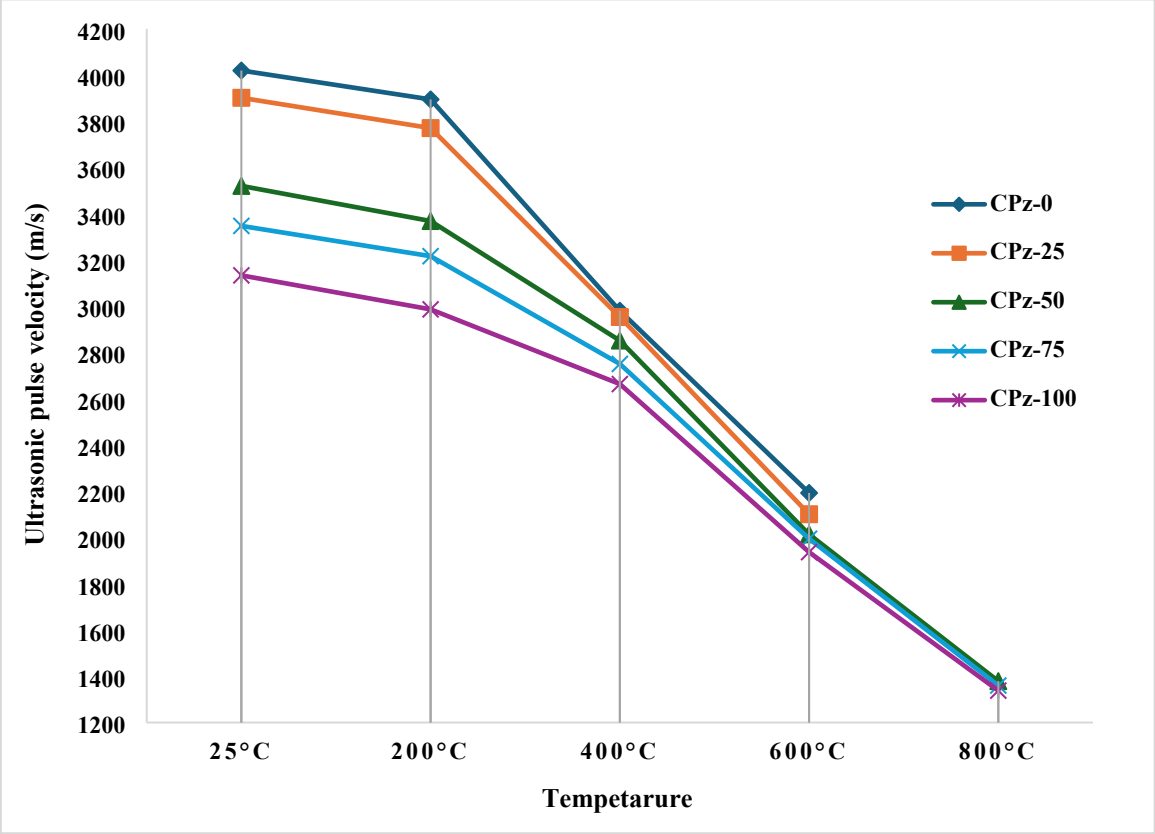

Fig. 8. Variations in ultrasonic pulse velocity of concrete with temperature at 28 days.

The relative evolution of the ultrasonic pulse velocity ($V_{T°}$ /$V_{25°}$) shows a more significant degradation with temperature in samples CP-z0 and CPz-25 compared to samples CPz-50, CPz-75, and CPz-100 (Fig. 9). The same behavior was observed for all samples up to 600 °C. At this temperature, CPz-0 samples undergo a significant decrease in velocity compared to the other samples. At a temperature of 600°C, the wave velocity of CPz-0 experiences a 50% reduction, while CPz-75 and CPz-100 demonstrate decreases of only 37.3% and 30%, respectively. Despite the higher porosity increase observed in PA when compared to NA, the rise in wave velocity for CPz-0 is more pronounced. This finding aligns with the compressive strength results and signifies a more robust bond between the paste and porous lightweight aggregates than with calcareous aggregates [22].

View Article Online
DOI: 10.1039/D5MA00680E

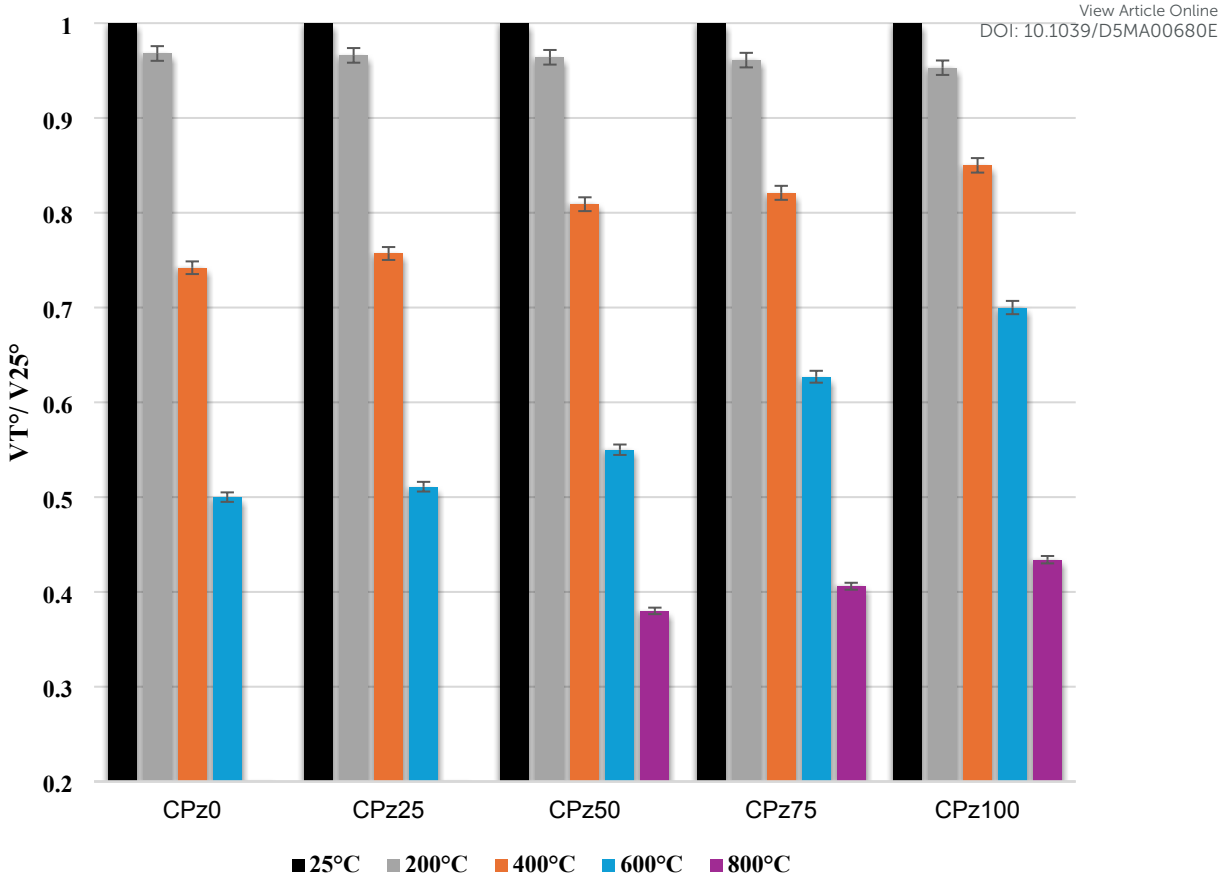

Fig. 9. Relative evolution of the ultrasonic pulse velocity of concrete as a function of temperature.

To understand the origin of the velocity increase, representative cross-sectional images of the thermally exposed samples were taken. At 400 °C, microcracks began to emerge, and the damage to the paste-aggregate interface was more pronounced in the CPz-0 sample compared to CPz-50 and CPz-100. With increasing temperatures up to 600 °C, a significant increase in deeper cracks in the cementitious matrix of CPz-0 was observed (Fig. 10). In addition, cracks through the interfacial zone between the normal aggregate and the cementitious matrix were observed in the CPz-0 sample, while the majority of cracks in the pozzolanic aggregate concrete are at the level of the cementitious matrix. This can be elucidated by the resilient interlocking sites formed between the paste and the aggregate, particularly during the penetration of the paste into the aggregate surface. As a result, a more robust connection between the paste and porous lightweight aggregates is established compared to calcareous aggregates [42].

View Article Online
DOI: 10.1039/D5MA00680E

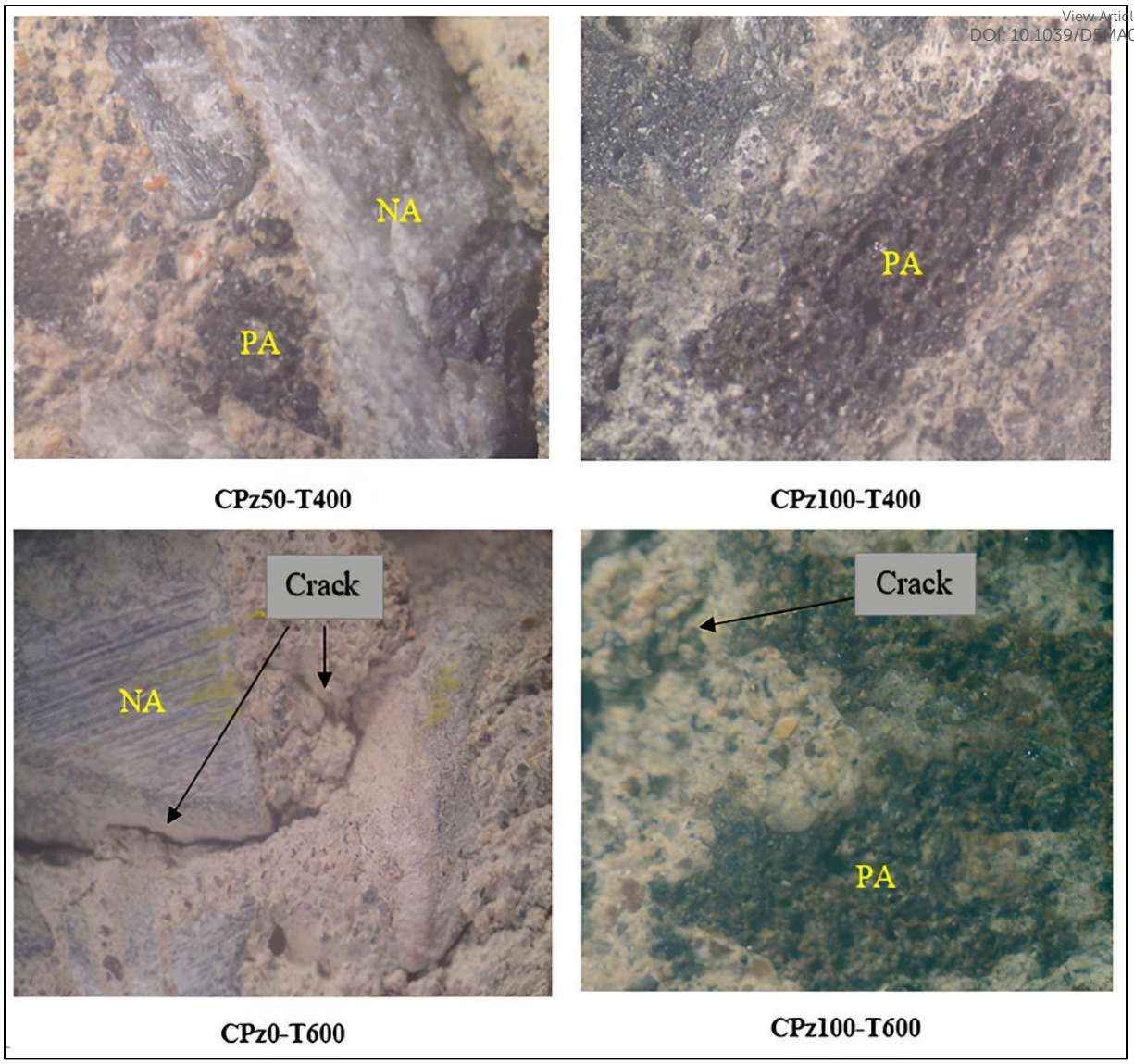

Fig. 10. Cross-sectional images after thermal exposure of concrete.

3.5 Relationships between relative residual compressive strength, pozzolan aggregate content and temperature.

The relative residual compressive strength is defined as the ratio of the residual strength at temperature f_T to the compressive strength at ambient temperature f_{25}. In the present work, a mathematical equation was developed through regression analysis to calculate the residual compressive strength relative to samples within the temperature range of 200 °C to 600 °C. However, a multiple regression analysis was performed, considering PA content and temperature as independent variables, while relative residual compressive strength was considered the dependent variable. The values of R-Square, relative residual compressive strength alongside the predictor variables are presented in Table 4. The R-Square obtained for

View Article Online
DOI: 10.1039/D5MA00680E

the multiple regression model was 0.86 (close to 1), indicating a high level of confidence and specifying a more reliable model.

Table 4. Mathematical correlations established for concrete blends.

Predictor variable	R-Square	Response parameter f_t/f_{25}	
Temperature (T) and pozzolan aggregate percentage (A)	0.86	(T=25°C)	1
		(200<T<600 and 0<A<100)	1.042-0.00087**T**-0.00183**A**

3.6 Thermo-mechanical parameters correlation

The complexity of the data forced us to use exploratory statistical methods. For each sample, the mechanical and physicochemical results were subjected to multivariate classification analyses.

The approach used in this case is principal component analysis (PCA) [30,31]. This method has been widely used in environmental and materials sciences [43–45]. In this study, the objective was to assess whether the overall thermal and mechanical properties of the various analyzed samples could be utilized to categorize distinct groups among raw materials, potentially associated with their composition. Additionally, the aim was to identify the most significant thermal and mechanical characteristics for differentiation. To achieve this, Principal Component Analysis (PCA) was conducted using correlation matrices. This procedure essentially involves normalizing each variable: each value is first shifted by subtracting the mean value and then scaled by dividing each shifted value by the standard deviation. The variables used in the present case is compressive strength, loss of mass, and ultrasonic pulse velocity as input variables.

View Article Online
DOI: 10.1039/D5MA00680E

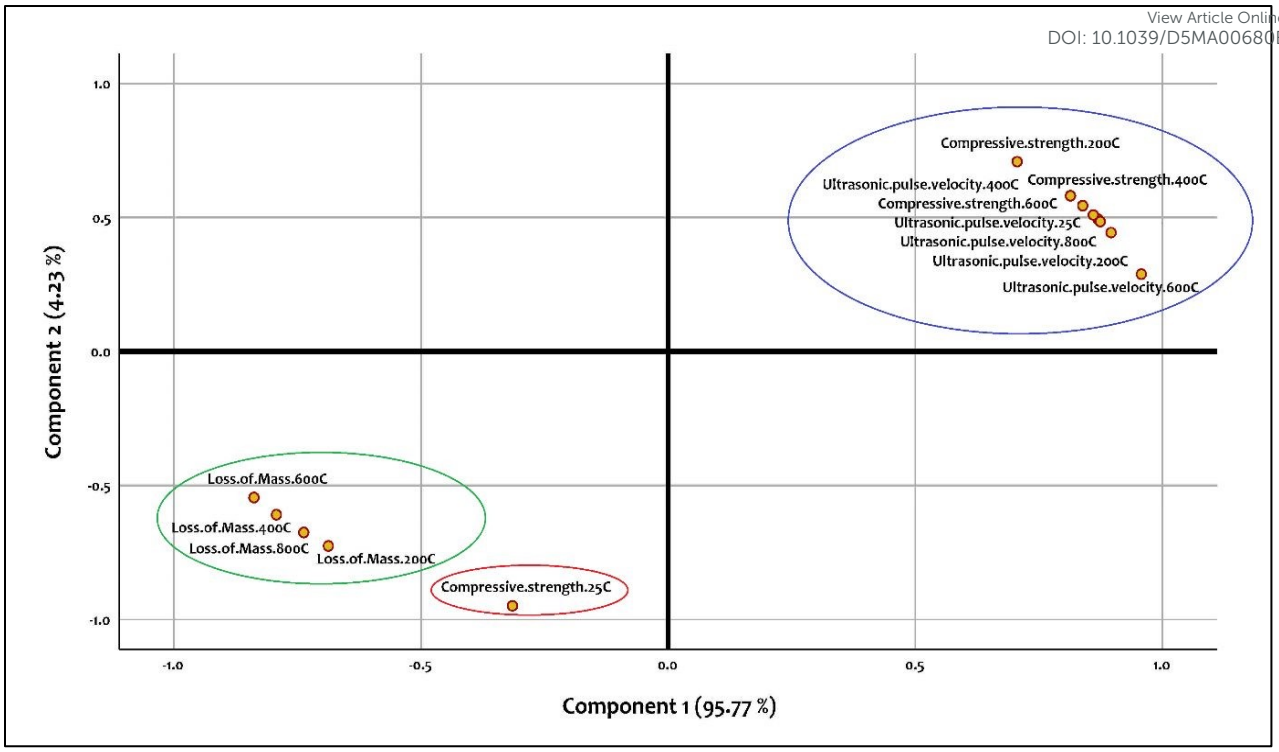

Fig. 11. Scatter plot obtained with correlation matrix.

The loading diagrams (Fig. 11) reveal that the first component (PC1) is predominantly influenced by mass loss, compressive strength, and UPV. In the PCA based on the correlation matrix, these factors cumulatively account for 95.77% of the variance in PC1. Conversely, the second component (PC2) is primarily influenced by room temperature compressive strength (25°C), with a less significant contribution of only 4.23%.

Upon reviewing Fig. 11, it is evident from the load diagram that the contributions of the different input variables to the two primary components lack distinct separation. Indeed, if we analyze the first axis, we can see that both the compressive strength of the samples and the ultrasonic pulse velocity are at negative PC1 values, confirming that the correlation between them is positive. This explains why compressive strength and ultrasonic pulse velocity show the same trend. Mass loss, on the other hand, is characterized by a negative correlation on the first axis.

From these results we can conclude that, the three variables have the same tendencies, it means that they are highly affected by the elevation of temperature, since we can see a high rate of variation in the first axis (95.77%) according to the PCA analysis. The difference, is that the variation of compressive strength and ultrasonic pulse velocity are positively oriented in this axis, which means that the changing in these parameters is the same, if the compressive strength decrease, consequently the ultrasonic decrease, while the rate of elevation of temperature increase. In contrast, the loss of mass is negatively correlated in the axis 1.

View Article Online
DOI: 10.1039/D5MA00680E

4. Conclusions

This research presents an experimental investigation aimed at evaluating the impact of elevated temperatures on the physical and mechanical properties of concrete using volcanic pozzolan (PA) as a substitute for natural aggregates (NA). The results indicate that:

- Increasing both the PA content and the temperature leads to a decrease in compressive strength and ultrasonic pulse velocity (UPV) values. However, the loss of strength decreases as the pozzolan replacement rate increases. At 800 °C, the compressive strength loss for CPz-0 (0 % PA) reaches 52 %, whereas CPz-100 (100 % PA) exhibits only 9 % loss.
- UPV is also better preserved in pozzolanic concretes: at 600 °C, the reduction in UPV is 50 % for CPz-0, 37.3 % for CPz-75, and 30 % for CPz-100, highlighting the stronger bond between the paste and pozzolanic aggregates.
- Natural aggregate concretes degrade rapidly above 400 °C, while concretes containing natural pozzolanic aggregates remain stable up to 600 °C. At 800 °C, CPz-0 specimens show severe degradation and concrete failure, whereas CPz-75 and CPz-100 retain 78 % and 91 % of their initial strength, with only limited microcracking.
- A clear correlation between relative residual compressive strength, PA content, and elevated temperature was established, confirming that pozzolan incorporation enhances mechanical and ultrasonic stability at high temperatures.

In conclusion, volcanic pozzolan significantly reduces the vulnerability of concrete to high temperatures while contributing to material sustainability through the valorization of a natural resource. Its incorporation represents an effective strategy to produce durable and fire-resistant concretes. Future work will focus on integrating fibers and mineral admixtures to further enhance mechanical and thermal performance.

Declaration of Competing Interest

The authors declare that they have no known competing financial interests or personal relationships that could have appeared to influence the work reported in this paper.

Data availability

Data will be made available on request.

References

View Article Online
DOI: 10.1039/D5MA00680E

[1] P.K. Mehta, P. Monteiro, Concrete: microstructure, properties, and materials, (No Title) (2006). https://cir.nii.ac.jp/crid/1130000797867624064 (accessed June 26, 2025).

[2] Z. Najeeb, M.A. Mosaberpanah, Mechanical and durability properties of modified High-Performance mortar by using cenospheres and Nano-Silica, Construction and Building Materials 362 (2023) 129782. https://doi.org/10.1016/j.conbuildmat.2022.129782.

[3] J. Zhang, J.L. Provis, D. Feng, J.S.J. Van Deventer, Geopolymers for immobilization of Cr6+, Cd2+, and Pb2+, Journal of Hazardous Materials 157 (2008) 587–598. https://doi.org/10.1016/j.jhazmat.2008.01.053.

[4] I. Janotka, S.C. Mojumdar, Thermal analysis at the evaluation of concrete damage by high temperatures, J Therm Anal Calorim 81 (2005) 197–203. https://doi.org/10.1007/s10973-005-0767-6.

[5] U. Schneider, Behaviour of concrete at high temperatures, Ernst, 1982.

[6] İ. Yüksel, R. Siddique, Ö. Özkan, Influence of high temperature on the properties of concretes made with industrial by-products as fine aggregate replacement, Construction and Building Materials 25 (2011) 967–972. https://doi.org/10.1016/j.conbuildmat.2010.06.085.

[7] A. Demez, M.B. Karakoç, Mechanical properties of high strength concrete made with pyrophyllite aggregates exposed to high temperature, Structural Concrete 22 (2021). https://doi.org/10.1002/suco.201900381.

[8] Ö. Sallı Bideci, The effect of high temperature on lightweight concretes produced with colemanite coated pumice aggregates, Construction and Building Materials 113 (2016) 631–640. https://doi.org/10.1016/j.conbuildmat.2016.03.113.

[9] M. Canbaz, The Effect of High Temperature on Concrete with Waste Ceramic Aggregate, Iran. J. Sci. Technol.Trans. Civ. Eng. 40 (2016) 41–48. https://doi.org/10.1007/s40996-016-0002-7.

[10] M. Yoon, G. Kim, G.C. Choe, Y. Lee, T. Lee, Effect of coarse aggregate type and loading level on the high temperature properties of concrete, Construction and Building Materials 78 (2015) 26–33. https://doi.org/10.1016/j.conbuildmat.2014.12.096.

[11] P. Turker, K. Erdogdu, B. Erdogan, Investigation of the various type of aggregate mortar exposed to fire, Journal of Cement Concrete World 6 (2001) 52–69.

[12] A. Neville, P.-C. Aïtcin, High performance concrete—An overview, Mat. Struct. 31 (1998) 111–117. https://doi.org/10.1007/BF02486473.

[13] A. Bellil, A. Aziz, I.-I. El Amrani El Hassani, M. Achab, A. El Haddar, A. Benzaouak, Producing of Lightweight Concrete from Two Varieties of Natural Pozzolan from the

Middle Atlas (Morocco): Economic, Ecological, and Social Implications, Silicon (2021). https://doi.org/10.1007/s12633-021-01155-8.

[14] A. Bellil, A. Aziz, M. Achab, A. Amine, H. El Azhari, Effects of the Variety and Content of Natural Pozzolan Coarse Aggregate on the Thermo-Mechanical Properties of Concrete, Biointerface Res. Appl. Chem 12 (2021) 5405–5415.

[15] A. Aziz, Structural and Physico-mechanical Investigations of New Acidic Geopolymers Based on Natural Moroccan Pozzolan: A Parametric Study, Silicon (2022) 1–12.

[16] A. Bellil, A. Aziz, I.-I. El Amrani El Hassani, M. Achab, A. El Haddar, A. Benzaouak, Producing of Lightweight Concrete from Two Varieties of Natural Pozzolan from the Middle Atlas (Morocco): Economic, Ecological, and Social Implications, Silicon 14 (2022) 4237–4248. https://doi.org/10.1007/s12633-021-01155-8.

[17] L. Turanli, B. Uzal, F. Bektas, Effect of large amounts of natural pozzolan addition on properties of blended cements, Cement and Concrete Research 35 (2005) 1106–1111. https://doi.org/10.1016/j.cemconres.2004.07.022.

[18] S. Ahmad, K.O. Mohaisen, S.K. Adekunle, S.U. Al-Dulaijan, M. Maslehuddin, Influence of admixing natural pozzolan as partial replacement of cement and microsilica in UHPC mixtures, Construction and Building Materials 198 (2019) 437–444. https://doi.org/10.1016/j.conbuildmat.2018.11.260.

[19] A. Aziz, A. Driouich, A. Bellil, M.B. Ali, S.E.L. Mabtouti, K. Felaous, M. Achab, A. El Bouari, Optimization of new eco-material synthesis obtained by phosphoric acid attack of natural Moroccan pozzolan using Box-Behnken Design, Ceramics International (2021) S0272884221025931. https://doi.org/10.1016/j.ceramint.2021.08.203.

[20] A. Aziz, O. Stocker, I.-E. El Amrani El Hassani, A.P. Laborier, E. Jacotot, A. El Khadiri, A. El Bouari, Effect of blast-furnace slag on physicochemical properties of pozzolan-based geopolymers, Materials Chemistry and Physics 258 (2021) 123880. https://doi.org/10.1016/j.matchemphys.2020.123880.

[21] M. Vafaei, A. Allahverdi, Influence of calcium aluminate cement on geopolymerization of natural pozzolan, Construction and Building Materials 114 (2016) 290–296. https://doi.org/10.1016/j.conbuildmat.2016.03.204.

[22] A. Aziz, A. Benzaouak, A. Bellil, T. Alomayri, I.-E.E. Ni el Hassani, M. Achab, H. El Azhari, Y. Et-Tayea, F.U.A. Shaikh, Effect of acidic volcanic perlite rock on physio-mechanical properties and microstructure of natural pozzolan based geopolymers, Case Studies in Construction Materials 15 (2021) e00712. https://doi.org/10.1016/j.cscm.2021.e00712.

View Article Online
DOI: 10.1039/D5MA00680E

[23] A. Aziz, A. Bellil, I.-E. El Amrani El Hassani, M. Fekhaoui, M. Achab, A. Dahrouch, A. Benzaouak, Geopolymers based on natural perlite and kaolinic clay from Morocco: Synthesis, characterization, properties, and applications, Ceramics International 47 (2021) 24683–24692. https://doi.org/10.1016/j.ceramint.2021.05.190.

[24] A. Aziz, I.-E. El Amrani El Hassani, A. El Khadiri, C. Sadik, A. El Bouari, A. Ballil, A. El Haddar, Effect of slaked lime on the geopolymers synthesis of natural pozzolan from Moroccan Middle Atlas, J Aust Ceram Soc 56 (2020) 67–78. https://doi.org/10.1007/s41779-019-00361-3.

[25] B. Achiou, H. Elomari, A. Bouazizi, A. Karim, M. Ouammou, A. Albizane, J. Bennazha, S. Alami Younssi, I.E. El Amrani, Manufacturing of tubular ceramic microfiltration membrane based on natural pozzolan for pretreatment of seawater desalination, Desalination 419 (2017) 181–187. https://doi.org/10.1016/j.desal.2017.06.014.

[26] A. Karim, B. Achiou, A. Bouazizi, A. Aaddane, M. Ouammou, M. Bouziane, J. Bennazha, S. Alami Younssi, Development of reduced graphene oxide membrane on flat Moroccan ceramic pozzolan support. Application for soluble dyes removal, Journal of Environmental Chemical Engineering 6 (2018) 1475–1485. https://doi.org/10.1016/j.jece.2018.01.055.

[27] NM 10.1.004. Hydraulic binders; Cements, Norme Marocaine, (2003)., (n.d.), (n.d.).

[28] H. Azidane, A. Benmohammad, B. Michel, M. El Bouhaddioui, Equilibrium beach profile on sandy beach of the Mehdya coast of Morocco, E3S Web Conf. 314 (2021) 03008. https://doi.org/10.1051/e3sconf/202131403008.

[29] A. Tahiri, A.E. Hassani, H.E. Hadi, Le patrimoine géologique du Maroc : l'exemple de la géodiversité paléozoïque de la région de Rabat, (2010).

[30] M.J. Baxter, C.E. Buck, Data handling and statistical analysis, CHEMICAL ANALYSIS-NEW YORK-INTERSCIENCE THEN JOHN WILEY- (2000) 681–746.

[31] I.T. Jolliffe, J. Cadima, Principal component analysis: a review and recent developments, Philosophical Transactions of the Royal Society A: Mathematical, Physical and Engineering Sciences 374 (2016) 20150202.

[32] W. Wongkeo, A. Chaipanich, Compressive strength, microstructure and thermal analysis of autoclaved and air cured structural lightweight concrete made with coal bottom ash and silica fume, Materials Science and Engineering: A 527 (2010) 3676–3684. https://doi.org/10.1016/j.msea.2010.01.089.

View Article Online
DOI: 10.1039/D5MA00680E

[33] D. Kore Sudarshan, A.K. Vyas, Impact of fire on mechanical properties of concrete containing marble waste, Journal of King Saud University - Engineering Sciences 31 (2019) 42–51. https://doi.org/10.1016/j.jksues.2017.03.007.

[34] H. Kitamura, M. Ueshima, S. Back, N. Sutthasil, H. Sakanakura, T. Ishigaki, M. Yamada, Impact of diatomite addition on lead immobilization in air pollution control residues from a municipal solid waste incinerator, Environ Sci Pollut Res 29 (2022) 21232–21243. https://doi.org/10.1007/s11356-021-17349-x.

[35] Q. Ma, R. Guo, Z. Zhao, Z. Lin, K. He, Mechanical properties of concrete at high temperature—A review, Construction and Building Materials 93 (2015) 371–383. https://doi.org/10.1016/j.conbuildmat.2015.05.131.

[36] M.S. Morsy, A.F. Galal, S.A. Abo-El-Enein, Effect of temperature on phase composition and microstructure of artificial pozzolana-cement pastes containing burnt kaolinite clay, Cement and Concrete Research 28 (1998) 1157–1163. https://doi.org/10.1016/S0008-8846(98)00083-0.

[37] M. Tufail, K. Shahzada, B. Gencturk, J. Wei, Effect of Elevated Temperature on Mechanical Properties of Limestone, Quartzite and Granite Concrete, International Journal of Concrete Structures and Materials 11 (2017) 17–28. https://doi.org/10.1007/s40069-016-0175-2.

[38] G. Roufael, A.-L. Beaucour, J. Eslami, D. Hoxha, A. Noumowé, Influence of lightweight aggregates on the physical and mechanical residual properties of concrete subjected to high temperatures, Construction and Building Materials 268 (2021) 121221. https://doi.org/10.1016/j.conbuildmat.2020.121221.

[39] H. Tanyildizi, M. Şahin, Application of Taguchi method for optimization of concrete strengthened with polymer after high temperature, Construction and Building Materials 79 (2015) 97–103. https://doi.org/10.1016/j.conbuildmat.2015.01.039.

[40] E. Hwang, G. Kim, G. Choe, M. Yoon, N. Gucunski, J. Nam, Evaluation of concrete degradation depending on heating conditions by ultrasonic pulse velocity, Construction and Building Materials 171 (2018) 511–520. https://doi.org/10.1016/j.conbuildmat.2018.03.178.

[41] L.C. de A. Mello, M.A. S. dos Anjos, M.V. V. A. de Sá, N. S. L. de Souza, E.C. de Farias, Effect of high temperatures on self-compacting concrete with high levels of sugarcane bagasse ash and metakaolin, Construction and Building Materials 248 (2020) 118715. https://doi.org/10.1016/j.conbuildmat.2020.118715.

[42] Y. Ke, S. Ortola, A.L. Beaucour, H. Dumontet, Micro-stress analysis and identification of lightweight aggregate's failure strength by micromechanical modeling, Mechanics of Materials 68 (2014) 176–192. https://doi.org/10.1016/j.mechmat.2013.09.005.

[43] A. Aziz, A. Driouich, M.B. Ali, K. Felaous, A. Bellil, B.B. Jindal, Improving the physicomechanical performance of geopolymer mortars using human hair as fibers: new horizons for sustainable applications, Environmental Science and Pollution Research (2023) 1–14.

[44] S.K. Rifi, L.E. Fels, A. Driouich, M. Hafidi, Z. Ettaloui, S. Souabi, Sequencing batch reactor efficiency to reduce pollutant in olive oil mill wastewater mixed with urban wastewater, International Journal of Environmental Science and Technology 19 (2022) 11361–11374.

[45] S.K. Rifi, S. Souabi, L. El Fels, A. Driouich, I. Nassri, C. Haddaji, M. Hafidi, Optimization of coagulation process for treatment of olive oil mill wastewater using Moringa oleifera as a natural coagulant, CCD combined with RSM for treatment optimization, Process Safety and Environmental Protection 162 (2022) 406–418.

Data Availability Statement

View Article Online
DOI: 10.1039/D5MA00680E

No new data were created or analyzed in this study. Data sharing is not applicable to this article.